universität wien

MASTERARBEIT / MASTER'S THESIS

Titel der Masterarbeit / Title of the Master's Thesis

„Estimation of competitive antagonist affinity of mAChR ligands from functional inhibition curves using Cheng-Prusoff equation"

verfasst von / submitted by

Dorka Fürtös BSc

angestrebter akademischer Grad / in partial fulfilment of the requirements for the degree of

Magistra pharmaciae (Mag.pharm.)

Wien, 2022 / Vienna 2022

Studienkennzahl lt. Studienblatt / degree programme code as it appears on the student record sheet:	UA 066 605
Studienrichtung lt. Studienblatt / degree programme as it appears on the student record sheet:	Masterstudium Pharmazie
Betreut von / Supervisor:	Ass.-Prof. Mag. Dr. Verena Pichler

ACKNOWLEDGEMENT

Firstly, I would like to thank my supervisor Ass.-Prof. Mag. Dr. Verena Pichler for the opportunity to perform my diploma thesis at the Department of Nuclear Medicine in the Vienna General Hospital. Thank you for introducing me to this very interesting research topic, thank you for your excellent supervision, constructive feedback, patience, kind support and unconditional help.

I would like to express my gratitude to my co-supervisor Ing. Dr. Marius Ozenil, BSc. MSc. for offering advice, encouragement and guidance throughout this project. Thank you for being there for me to solve every challenge professionally.

Furthermore, I would like to thank Dipl.-Ing. Jonas Kilian, BSc. MSc. for the synthesis of the test compounds and for assisting me in cell culture.

I would like to pay my special regards to the entire working group of the Department of Nuclear Medicine for their warm welcome, helping me find my way around and for always answering my questions.

Finally, I would like to express my deepest gratitude to my family, friends, colleagues and my boyfriend for supporting and encouraging me endlessly throughout my studies and this thesis.

ABSTRACT

Muscarinic acetylcholine receptors (mAChRs) regulate essential functions of the central (CNS) and peripheral nervous systems (PNS). Signal transduction through these receptors has been associated with various neurological disorders like Alzheimer's disease and schizophrenia. An efficient biological testing regime is the current strategy to investigate potential drug candidates that are more subtype selective. Therapeutic and diagnostic application of potentially selective mACh ligands could contribute to clinical disease management and treatment of neurological and psychiatric disorders and diseases. Identification of these ligands is difficult due to the similarity of the orthogonal ligand binding sites between the five receptor subtypes.

Antagonist assessment was performed by a competitive radioligand binding assay, a method for measuring the affinity of sixteen newly synthesized ligands targeting a receptor of interest. Different concentrations of the test ligands with a fixed concentration of the radiolabelled competitor [N-methyl-^{3}H] scopolamine methyl chloride ([^{3}H] NMS) were incubated with membrane preparations prepared from Chinese hamster ovary cells (CHO) transfected with each of the mAChR subtypes as the source of the receptors. The bound and unbound ligands were separated using a cell harvester with GF/B glass fibre filter paper. The data from the experiments were mathematically analysed using the computer programme GraphPad Prism to determine the specific binding values. The K_i value was calculated using the IC_{50} value according to the Cheng-Prusoff equation.

In conclusion, the most promising candidates in terms of binding affinity are ARA 54 and ARA 55. Both compounds demonstrated excellent results with K_i values in the low nanomolar range for the M_1, M_4 and M_5 receptors. Other good binding properties were performed by ARA 35, ARA 56, ARA 122, ARA 156 and RR 41. Compound MIMA 174 was the only test ligand that showed better binding affinity towards the M_3 subtype, whereas all the other important compounds favoured the M_1 receptor. When comparing the K_i values of other subtypes with M_1 the ratio is often not high enough to indicate M_1 subtype selectivity. Nevertheless, the affinities in the low nanomolar range make these compounds interesting candidates for further development.

ZUSAMMENFASSUNG

Muskarinische Acetylcholinrezeptoren regulieren wesentliche Funktionen des zentralen und peripheren Nervensystems. Die Signalübertragung durch diese Rezeptoren wurde mit verschiedenen neurologischen Störungen, wie Alzheimer und Schizophrenie in Verbindung gebracht. Ein effizientes biologisches Testregime ist die aktuelle Strategie, um potenzielle Wirkstoffkandidaten zu analysieren, die selektiver auf die unterschiedlichen Subtypen sind. Die therapeutische und diagnostische Anwendung potenziell selektiver Liganden könnte zum klinischen Krankheitsmanagement und zur Behandlung von neurologischen und psychiatrischen Störungen beitragen. Die Identifizierung dieser Liganden ist aufgrund der Ähnlichkeit der orthosterischen Ligandenbindungsstellen zwischen den fünf Rezeptorsubtypen schwierig. Die Analyse von Antagonisten erfolgt durch einen kompetitive Radioliganden-Bindungsassay, ein Verfahren zur Messung der Affinität neu synthetisierter Liganden. Für diesen Assay werden Zellmembranen aus chinesischen Hamstereierstockzellen gewonnen, die mit jeweiligen humanen mAChR Subtypen transfiziert werden. Unterschiedliche Konzentrationen der Testliganden wurden mit [N-Methyl-^{3}H] scopolaminmethylchlorid und den Membranpräparationen inkubiert. Gebundene und ungebundene Liganden wurden mit einem Zellernter mit GF/B-Glasfaserfilterpapier getrennt. Die Daten aus den Experimenten wurden mathematisch mit dem Computerprogramm GraphPad Prism analysiert, um die spezifischen Bindungswerte zu bestimmen. Der K_i-Wert wurde mit dem IC_{50}-Wert nach der Cheng-Prusoff-Gleichung berechnet.

Zusammenfassend sind die vielversprechendsten Kandidaten in Bezug auf die Bindungsaffinität ARA 54 und ARA 55. Beide Verbindungen zeigten hervorragende Ergebnisse mit K_i-Werten im niedrigen nanomolaren Bereich mit den M_1, M_4 und M_5 Rezeptoren. Weitere gute Bindungseigenschaften zeigten ARA 35, ARA 56, ARA 122, ARA 156 und RR 41. Die Verbindung MIMA 174 war der einzige Testligand, der eine bessere Bindungsaffinität zum M_3 Subtyp zeigte, während alle anderen wichtigen Verbindungen den M_1 Rezeptor bevorzugten. Beim Vergleich der K_i-Werte anderer Subtypen mit M_1 ist das Verhältnis oft nicht hoch genug, um eine Selektivität des M_1 Subtyps anzuzeigen. Nichtsdestotrotz sind diese Verbindungen aufgrund ihrer hohen Affinität im nanomolaren Bereich interessante Kandidaten für die weitere Entwicklung.

TABLE OF CONTENT

1 INTRODUCTION

1.1 G PROTEIN COUPLED RECEPTORs

G protein coupled receptors (GPCRs) represent the largest family of human membrane bound proteins. [1] They are proteins with seven transmembrane domains that convert extracellular signals into intracellular responses and thus regulate intracellular signalling cascades. They can be stimulated by hormones, neurotransmitters, ions, and others. [2,3] Drugs can induce, block, or modulate the receptors, thereby altering the intracellular signalling profile of the receptors, making GPCRs ideal drug targets. [1] Currently, 34% of small molecule drugs bind to these receptors (Figure 1). [4]

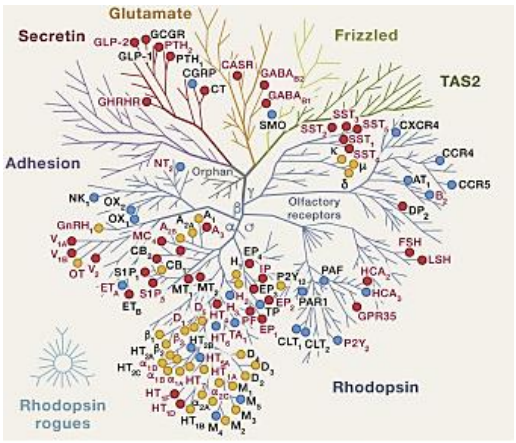

Figure 1: GPCRs targeted by Food and Drug Administration (FDA) approved drugs. [4]

As the name implies, GPCRs interact with G proteins in the plasma membrane. The heterotrimeric G proteins consist of three subunits: G_α, G_β, and G_γ. G proteins have the ability to bind guanosine triphosphate (GTP) and guanosine diphosphate (GDP). In the absence of a signal, G_α binds GDP, therefore G_α associates with G_β and G_γ and they form an inactive heterotrimer. When a signal molecule activates the GPCR, receptor mediated activation of the G proteins occurs. The receptor changes its conformation, GTP replaces GDP, and the G_α dissociation from the $G_{\beta\gamma}$ subunits follows. Each subunit modulates the activity of various downstream effector proteins. [2,5] Hydrolysis of GTP to GDP by the intrinsic GTPase activity of the G_α subunit terminates signalling. G_α then associates with $G_{\beta\gamma}$, also binding GDP, and the cycle is completed. [2,3]

1.2 mACh RECEPTORs

Acetylcholine (ACh) was the first molecule identified as a neurotransmitter. It binds two types of receptors: the ionotropic family of nicotinic acetylcholine receptors (nAChR) and the metabotropic family of muscarinic acetylcholine receptors (mAChR), first classified by Sir Henry Dale in 1914. Both belong to the family of GPCRs. [6,7] There are six classes of GPCRs, which are distinguished on the basis of amino acid sequence similarities. mAChRs belong to class A, also called rhodopsin-like receptors, which contains the largest number of GPCRs in humans. [4]

mAChRs are present in many organs and tissues, with individual subtypes dominating. They regulate essential functions of the central and peripheral nervous systems, as well as non-neuronal effects of ACh (Table 1). [8-10] These physiological functions include motoric and cognitive functions, smooth muscle contraction as well as cell differentiation and immune functions. [7-10] Today, there are five subtypes of mAChRs that differ in their distribution, signalling pathways, and physiological functions: M_1, M_2, M_3, M_4, and M_5. [8-10] The variability between them is limited to the carboxy and amino terminals and to the third cytoplasmic loop of the proteins. [7]

Table 1: mAChRs are involved in many physiological functions in different areas of the human body. The main area of action is in the central and peripheral nervous system. [7-10]

Region	**Physiological function**
Central nervous system (CNS)	cognitive-, behavioural-, motoric- and autonomic function, temperature and cardiovascular regulation, memory
Peripheral nervous system (PNS)	vegetative processes: regulating cardiac rate and force, smooth muscle contraction, exocrine and endocrine glandular secretion
Non-neuronal	cell proliferation, differentiation, apoptosis, migration of cells, angiogenesis, immune functions

The M_1 receptor subtype is mainly found in the CNS and ganglia. It is involved in memory and learning processes. M_2 receptors are found to a great extent in the heart, while the M_3 subtype is involved in smooth muscle contraction. M_4 receptors function predominantly in the forebrain, hippocampus and striatum, and are associated with pain processes. The M_5 receptor subtype is thought to be involved in microcirculation in the brain and regulates vasoconstriction and vasodilation. [7,10,11]

The structures of mAChRs resemble the overall folding of other GPCRs, which is characterized by a single protein molecule spanning the plasma membrane and having seven hydrophobic transmembrane domains connected by three extracellular and three intracellular hydrophilic loops. [8,13] The ligand recognition site is located in the outer half of the membrane. [10] Three types of ligands can be distinguished in mAChRs. There are orthosteric, allosteric, and bitopic ligands. Orthosteric ligands bind at the same site as ACh and have a high affinity for the receptor. These ligands can be agonists, antagonists, and inverse agonists. [12] The binding pocket of the orthosteric ligand is buried deep in the membrane (Figure 2). These ligands make hydrophobic contact with the receptor whereas smaller number of polar contacts are also important for binding. [8] An example of an orthosteric ligand would be tiotropium, a nonselective antagonist for the mAChR.

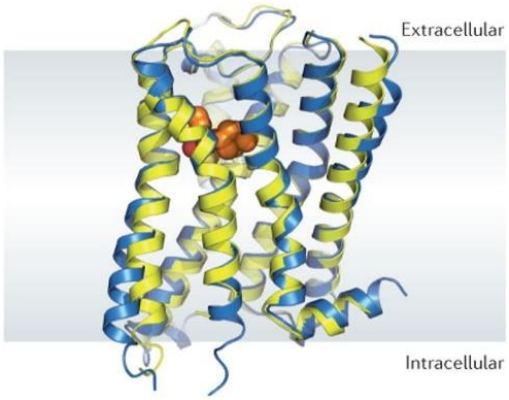

Figure 2: Structure of the M_3 mAChR subtype. The orange ligand represents tiotropium, an antagonist that binds to the orthosteric ligand binding pocket. [8]

Allosteric ligands have a different binding site. They have high selectivity for the receptor subtype but limited receptor affinity. These ligands can be positive, negative, and neutral allosteric modulators that regulate the affinity of orthosteric ligands. Examples for allosteric modulators are gallamine and alcuronium, both used as muscle relaxants.

Bitopic ligands bridge both binding sites of the receptor, therefore they have high subtype selectivity while maintaining high affinity for the receptor. [12]

mAChRs signal through both G protein and β-arrestin cascades. [9] The odd-numbered muscarinic receptors, M_1, M_3, and M_5, couple to $G_{\alpha q/11}$, which is a stimulatory pathway, whereas the even-numbered receptors, M_2 and M_4, activate $G_{\alpha i/o}$, an inhibitory signalling cascade (Figure 3). [8,9,10]

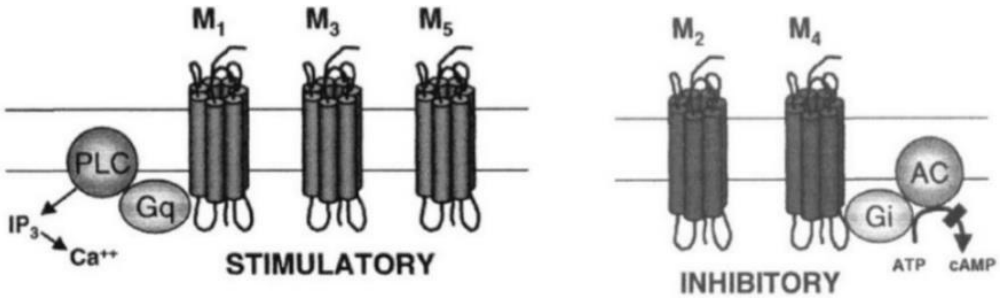

Figure 3: An overview of the five different mAChR subtypes and their signalling pathways. [7]

An important sequence difference in the third internal loops between the even and odd subtype sequences probably determines the specific coupling preferences of these two groups. [10] Signal via the $G_{\alpha q/11}$ pathway leads to stimulation of phospholipase C (PLC). This results in diacylglycerol (DAG) and inositol triphosphate (IP_3) from cleavage of phosphatidylinositol bisphosphate (PIP_2). IP_3 causes intracellular Ca^{2+} mobilisation from the endoplasmic reticulum (ER), whereas DAG activates PKC, leading to phosphorylation of numerous proteins.

The α-subunit of the G protein inhibits adenylyl cyclase (AC) after activation of $G_{i/o}$ signalling and decreases cyclic adenosine monophosphate (cAMP) levels. The βγ-dimer stimulates inwardly rectifying K^+ channels and inhibits voltage-gated Ca^{2+} channels. This leads to hyperpolarization and a decrease in cell membrane excitability. [3,9,13]

A well-established mechanism of desensitisation of GPCRs can be achieved by arrestins, proteins that modulate G protein signalling. They bind to the phosphorylated portion of the receptor and prevent the receptor from interacting with G proteins by physically blocking the nucleotide exchange factor, which leads to cessation of signal transduction and also initiates internalisation of the receptor. [5,9]

1.3 POTENTIAL IN MEDICAL IMAGING AND TREATMENT

Signal transduction via mAChRs has been associated with various CNS and PNS disorders like schizophrenia, Alzheimer's and Parkinson's disease. [7,9] Drug development to treat these disorders is considered a major challenge because the biology underlying certain diseases is not well understood. Positron emission tomography (PET) has already led to improved knowledge of the pathophysiology of many CNS disorders and can be used for differential diagnosis, leading to more accurate information on prognosis, management, and treatment. It can contribute to observing alterations in expression levels of neuroreceptors in the pathogenesis of diseases. [15,16] PET is the method of choice for non-invasive functional imaging. It is based on the tracer principle using small amounts of specific radiopharmaceuticals. Changes in metabolism, blood flow, and regional chemical composition can be analysed. PET allows quantification and visualisation of biochemical processes by monitoring the time-dependent distribution of these radiotracers labelled with short-lived positron-emitting isotopes, like carbon-11, fluorine-18 and gallium-68. [14-18]

Radiotracers in neurology are often compounds that bind with high selectivity to a specific molecular target such as a receptor or enzyme. [14] Pharmacologically active compounds may also be used but only below the pharmacologically active dose. [12] Radiotracers that bind to dopaminergic, serotonergic, and cholinergic receptors are used to study the role of these hormones in mental disorders. [15] A radiotracer that targets the CNS must be able to cross the blood-brain barrier (BBB), should bind the target with high affinity and selectivity and must also have physicochemical and pharmacological properties that allow radiolabelling and safe administration to humans. [12,14] PET tracers targeting the CNS are radiolabelled using carbon-11 or fluorine-18. [14] An example for this is the alkylation with [^{11}C] methyl iodide, to produce [^{11}C] raclopride, a widely used radiotracer targeting dopamine receptors. [17] (Figure 4) Radionuclides are prepared in a cyclotron by irradiating ^{14}N, ^{16}O, and ^{18}O with low and intermediate energy protons (H^+) on the day of use. [19] The modifications with covalently bound radionuclides leave the chemical structures unchanged or only slightly altered so that the behaviour of the molecule does not change. [14,19]

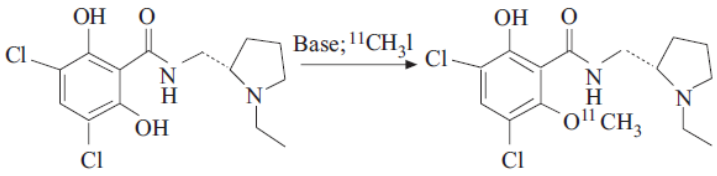

Figure 4: Alkylation with [^{11}C] methyl iodide, a modification with covalently bound radionuclide, to produce [^{11}C] raclopride. [17]

Radiotracers are administered in nanomolar concentrations. This concept of micro dosing reduces adverse effects, such as addictive and neurotoxic effects. [12,14] Radiotracers are typically injected intravenously, but they can also be swallowed or inhaled depending on the site of interest. [15] The radiotracer's unstable nuclei emit positrons, which interact with electrons. Due to this encounter, both, the positron and the electron, annihilates producing two 511 keV gamma rays that are released in opposite directions (180°) and can be detected by the scanner. A computer then uses this data to create a 3D image of the tracer in the body (Figure 5). [15]

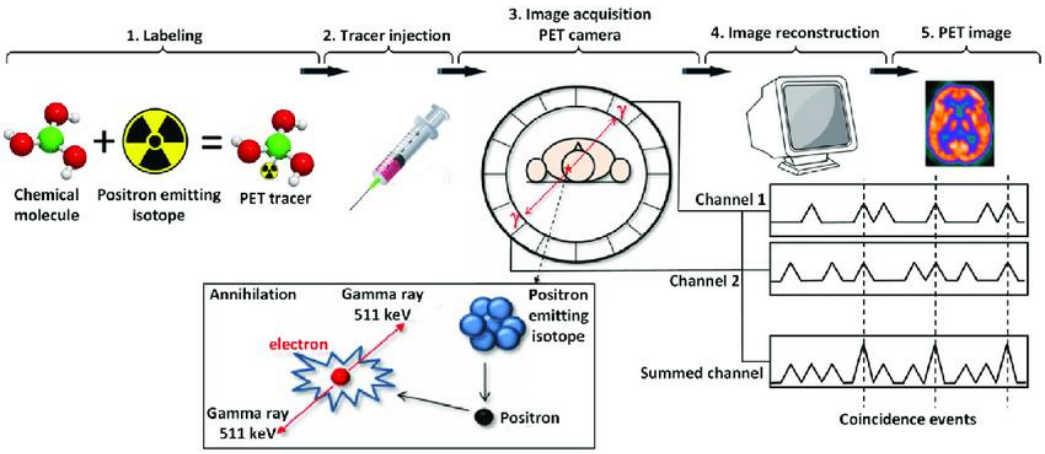

Figure 5: An overview of the process of producing and applying the tracer, detectors measuring the gamma rays and converting the data to tomographic images. [21]

A suitable PET tracer could elucidate the natural functions of mAChR regulation, which would have enormous impact on clinical disease management. However, so far, no mAChR PET tracer is clinically applied. [12] The majority of potential small molecule PET tracers designed to map mAChRs in the CNS and PNS have failed in preclinical development. They exhibit a lack of selectivity, slow kinetics, or low specific binding. The major problem is the similarity of the orthosteric binding pockets of the mAChR subtypes. [12,20]

Therapeutic application of potential selective mAChR ligands could contribute to treatment in areas such as Alzheimer's disease, disorders of intestinal motility and urinary bladder function. [10] Selective agonists and antagonists have the greatest therapeutic potential in the treatment of neurologic and psychiatric disorders and diseases (Table 2). [7-9]

Table 2: Diseases and potential treatment methods with selective mAChR agonists and antagonists. [8]

Disease	Potential treatment method
Alzheimer's disease	M_1- selective receptor agonists
Schizophrenia	M_1- and M_4- selective receptor agonists
Drug addiction	M_5- selective receptor antagonists
	M_1- and/or M_4- selective receptors agonists
Type 2 diabetes	M_3- selective receptor agonist
Cancer	M_1- and M_3- selective receptor antagonists

Antagonists bind to mAChRs in both the active and inactive states, whereas agonistic ligands bind only to receptors in the high affinity, active state. [20] Identification of subtype selective ligands for mAChRs is difficult because of the similarity of ligand binding sites among the five subtypes.

1.4 COMPETITIVE BINDING ASSAY

Competitive binding assays are the principal method for measuring the affinity of a targeting ligand for a receptor of interest. [21] These assays allow for the kinetic profiling of a ligand at a given receptor in the early stages of drug development and discovery. [22] For PET radiotracer the K_i value representing binding affinity should be in the low nanomolar range. If the binding affinity is not sufficiently high, such a drug may not be useful. [23] Competition occurs between increasing concentrations of the test ligand and a fixed concentration of a well-characterized radioligand (Figure 7). [21,25]

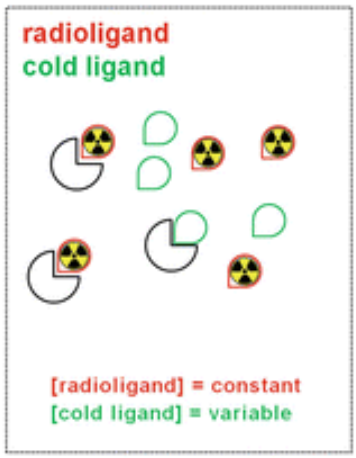

Figure 6: Illustration of the competition between radioligand and test ligand for the receptor. [30]

Radioactive assays are rapid, easy to use, and reproducible, but they are hazardous to human health, generate radioactive waste, require special laboratory conditions, and are more expensive. There are also nonradioactive assay technologies. Nonradioactive assays are based on optical methods such as fluorescence polarization or energy transfer. [24,26]

For the here applied experiments, a preparation containing the receptor is needed. This is usually a membrane suspension in aliquots prepared from cell lines. [21,25] Suitable labelled ligands commonly used to measure muscarinic receptor binding include [^{3}H] midafenacin, [^{3}H] uinuclidinyl benzilate ([^{3}H] QNB), and [N-methyl-^{3}H] scopolamine methyl chloride ([^{3}H] NMS). [27,29]

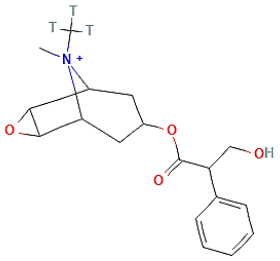

Figure 7: Structure of [N-methyl-^{3}H] scopolamine methyl chloride. [29]

Aliquots of the membrane preparation are incubated with selected concentrations of the radioligand and the test ligand for a specified time, temperature and buffer concentration. [25] Separation of bound from free ligand present in the mixture is accomplished by rapid filtration through glass fibre filter paper. [21] GF/B filters are pre-treated with 0.05-0.125% polyethyleneimine (PEI) solution prior to use, which creates a positive surface charge that helps trap negatively charged membrane fragments. [25]

Cell-based radioligand binding assays are frequently affected by inconsistencies. Variability in target protein expression due to intercellular heterogeneity and interlaboratory differences in cell line origin and passage can adversely effect reproducibility. [28] Additives like dimethyl sulfoxide (DMSO), dimethylformamide, acetonitrile, and alcohols may interfere with some receptor binding assays. Serial dilutions should be checked to ensure that precipitation has not occurred. [21]

Data from experiments are analysed mathematically to determine specific binding values. [25,26,31] Classically, binding affinity is expressed by the equilibrium dissociation constant (K_D), inhibition constant (K_i), or half maximum inhibition concentration (IC_{50}). [23]

Understanding the theory of receptor-ligand interactions is essential for planning, performing, analysing, and interpreting binding experiments. [25] The binding interaction between a ligand and a receptor can be described by equation 1. L represents the free ligand, R represents the unbound receptor, and LR represents the bound ligand-receptor complex. [25,26] There is a dynamic exchange between bound and unbound states described by the association and dissociation constants k_{on} and k_{off}. [25,26]

$$R + L \underset{koff}{\overset{kon}{\rightleftharpoons}} RL$$

Equation 1: This equation describes receptor-ligand binding interaction. R: unbound receptor, L: free ligand, k_{on}: association constant, k_{off} dissociation constant RL: receptor-ligand complex.

Two criteria for a successful binding experiment are important: the reactions must be in equilibrium at the time of measurement, and the concentration of a reactant must be varied. [32]

At equilibrium, the rates of forward and backward reactions are equal. [26] Equation 2 describes the equilibrium association constant K_a.

$$\frac{[RL]}{[R][L]} = \frac{k_{on}}{k_{off}} = K_a$$

Equation 2: This equation describes the equilibrium association constant K_a. RL: receptor-ligand complex, R: unbound receptor, L: free ligand, k_{on}: association constant, k_{off} dissociation constant, K_a: equilibrium association constant.

In binding assays, the equilibrium dissociation constant described in equation 3 is more important than the equilibrium association constant. It is the inverse of K_a and a measure of the tendency of the receptor-ligand complex to dissociate. [25,26]

$$\frac{[R][L]}{[RL]} = \frac{k_{off}}{k_{on}} = K_D$$

Equation 3: The equation describes the equilibrium dissociation constant K_D. R: unbound receptor, L: free ligand, RL: receptor-ligand complex, k_{off} dissociation constant, k_{on}: association constant, K_D: equilibrium dissociation constant.

If the concentration of competitive test ligand is varied and both the receptor concentration and radioligand concentration are held constant, inhibition curves, smooth sigmoidal curves, can be generated using a dedicated computer program for radioligand binding analysis such as Prism from GraphPad. [21,24,31,33] Using this computer program the data are analysed with a nonlinear regression curve. [34] From the fitted curve, the IC_{50} for the test ligand can be calculated, which represents the analyte concentration that displaces 50% of the bound labelled ligand. [24,31,33,34]

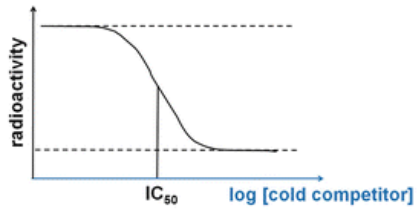

Figure 8: Schematic inhibition curve with the IC_{50} value determined. [24]

The half-maximal inhibitory concentration (IC_{50}) is the most commonly used measure, as it is a concise and interpretable summary of a drug's activity, which conveys an indication of the drug's potency, but unlike K_i values, it is assay-specific and comparable only under certain conditions. [35-37]

K_i, the inhibitor constant, can be calculated using the IC_{50} according to the Cheng-Prusoff equation, which is shown in equation 4. [36,37]

$$K_i = \frac{IC_{50}}{1 + \frac{[L]}{K_D}}$$

Equation 4: The Cheng-Prusoff equation defines the relation between the K_i and the IC_{50} of an inhibitory ligand. K_i: inhibitor constant, IC_{50}: half-maximal inhibitory concentration, L: inhibitory ligand, K_D: equilibrium dissociation constant of the radioligand.

Equation 4 assumes that both agents compete with each other in a reversible manner at a single site according to the law of mass action, that the reaction is in equilibrium, and that the free concentrations of the agents are known and constant throughout the experiment. The K_D value of the radioligand must also be known. [38] K_D values for the radioligand [N-methyl-^{3}H] scopolamine methyl chloride defined in literature are shown in table 3.

Table 3: K_D values of the radioligand [N-methyl-^{3}H] scopolamine methyl chloride from literature.

mAChR subtype	M1	M2	M3	M4	M5
K_D [nM]	0.17	0.15	0.16	0.07	0.16

Both low IC_{50} and K_i values imply high binding affinity. [23] A suitable selectivity profile coupled with a sufficiently high affinity (ca. 1-50 nM) is essential as only compounds with a K_i value in the low nanomolar range are of importance for PET radiotracer development. [39] Although in vitro assays represent an inexpensive and quick method of assaying new probes for bioactivity it is impossible, in a membrane suspension, to reproduce the cellular environment of receptors of a living cell. [25,40]

2 AIM

Selective mAChR ligands could have tremendous impact on clinical treatment of diseases, but their development is difficult due to the similarity of the ligand binding site of all five receptor subtypes. The aim of this master's thesis was to investigate the binding properties of sixteen potential mAChR antagonists in competitive radioligand binding experiments. The desired outcome was a suitable selectivity profile in combination with a sufficiently high affinity with a K_i value in the low nanomolar range.

In vitro experiments included incubation of the sixteen test ligands with [^{3}H] NMS as radioligand and membrane preparations of CHO cells transfected with each muscarinic receptor subtype. The measured data were analysed using the computer programme GraphPad Prism. The K_i value was calculated using the IC_{50} value according to the Cheng-Prusoff equation. The binding experiments serve as a selection procedure, so the results show which candidates would be most promising for further experiments and development.

3 MATERIALS

3.1 CHEMICALS

- [N-Methyl-^{3}H] Scopolamine Methyl Chloride ([^{3}H] NMS)
- Dimethyl Sulfoxide (DMSO)
- Dulbecco's Phosphate Buffered Saline (DPBS)
- Ethylenediaminetetraacetic Acid (EDTA)
- F-12 Nutrient Mixture (Ham)
- Fetal Bovine Serum (FBS)
- Geniticin
- Hydrochloric Acid (HCl)
- L-Glutamine
- Magnesium Chloride Anhydrous ($MgCl_2$)
- Poly (Ethyleneimine) Solution (PEI)
- Protease Inhibitor P2714
- Scopolamine
- Stable Transfected Cell Line (CHO – K1), M_{1-5} Muscarinic Receptor (Human), Wild Type
- Tris (Hydroxymethyl) Aminomethane (TRIS)
- Trypsin
- Ultima Gold^{tm} Scintillation Cocktail

3.2 EQUIPMENT

- Cell Harvester - Brandel
- Beta Counter Hidex 300SL
- Centrifuge
- Ultracentrifuge

3.3 SOFTWARE

- GraphPad Prism 8.2.1
- Microsoft Office
- Mikro Win 2000

3.4 TEST LIGANDS

Table 4: Chemical structures and parameters of the sixteen test ligands for the competitive radioligand binding experiments.

ARA 35 Chemical Formula: $C_{19}H_{20}F_2N_2O_2$ Molecular Weight: 346.38 clogP: 3.14	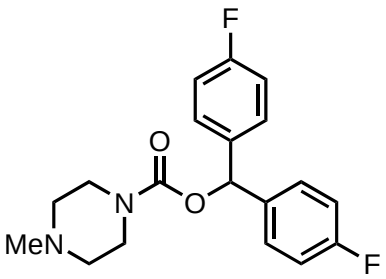
ARA 54 Chemical Formula: $C_{20}H_{22}F_2N_2O_2$ Molecular Weight: 360.41 clogP: 2.44	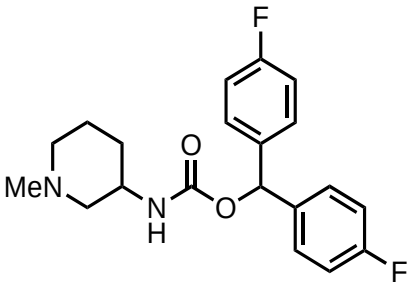
ARA 55 Chemical Formula: $C_{20}H_{22}F_2N_2O_2$ Molecular Weight: 360.41 clogP: 3.19	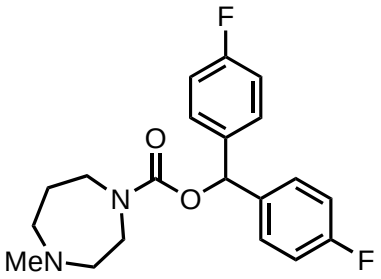
ARA 56 Chemical Formula: $C_{21}H_{22}F_2N_2O_2$ Molecular Weight: 372.42 clogP: 1.92	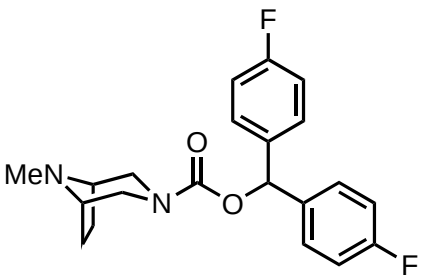

ARA 117 Chemical Formula: $C_{20}H_{22}F_2N_2O_2$ Molecular Weight: 360.41 clogP: 1.12	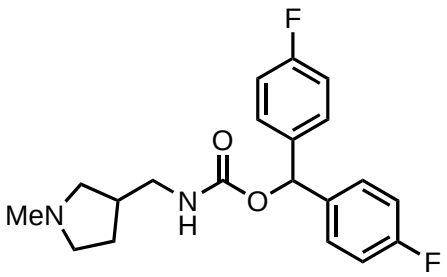
ARA 122 Chemical Formula: $C_{21}H_{22}F_2N_2O_2$ Molecular Weight: 372.42 clogP: 2.08	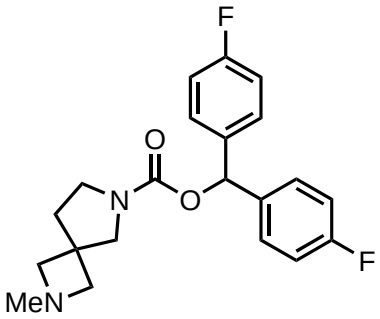
ARA 154 Chemical Formula: $C_{23}H_{24}F_2N_2O_2$ Molecular Weight: 398.45 clogP: 2.31	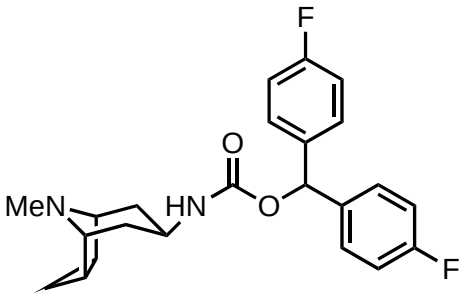
ARA 156 Chemical Formula: $C_{20}H_{20}F_2N_2O_2$ Molecular Weight: 358.39 clogP: 1.37	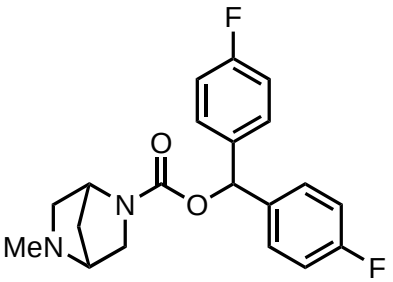

ARA 166 Chemical Formula: $C_{19}H_{20}F_2N_2O_2$ Molecular Weight: 346.38 clogP: 1.77	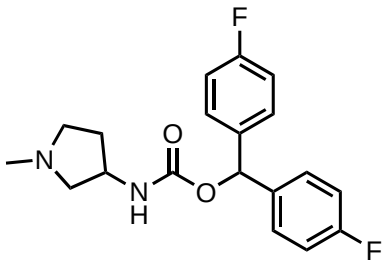
MIMA 174 Chemical Formula: $C_{21}H_{23}N_3O$ Molecular Weight: 332.44 clogP: 3.78	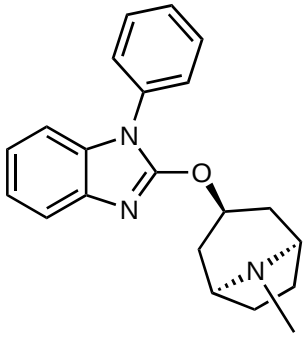
MIMA 195 Chemical Formula: $C_{21}H_{21}N_3O_2$ Molecular Weight: 347.41 clogP: 2.69	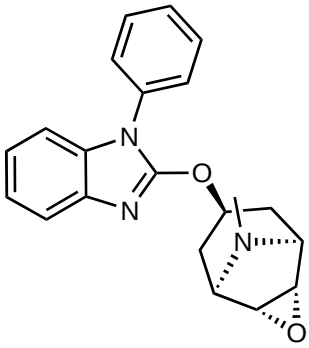
RR 37 Chemical Formula: $C_{18}H_{20}N_2O_2$ Molecular Weight: 296.37 clogP: 3.10	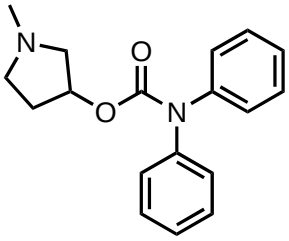

RR 39 Chemical Formula: $C_{19}H_{22}N_2O_2$ Molecular Weight: 310.40 clogP: 3.78	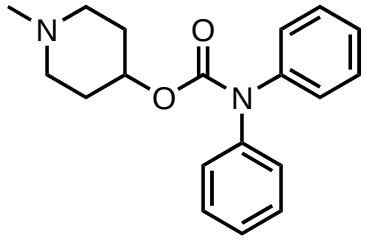
RR 40 Chemical Formula: $C_{17}H_{18}N_2O_2$ Molecular Weight: 282.34 clogP: 3.01	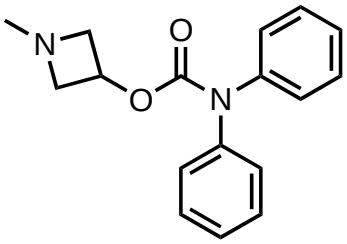
RR 41 Chemical Formula: $C_{21}H_{24}N_2O_2$ Molecular Weight: 336.44 clogP: 4.10	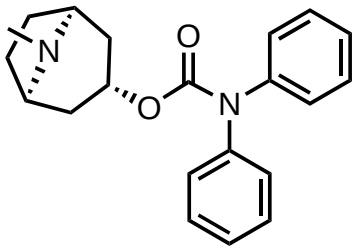
RR 43 Chemical Formula: $C_{21}H_{22}N_2O_3$ Molecular Weight: 350.42 clogP: 4.01	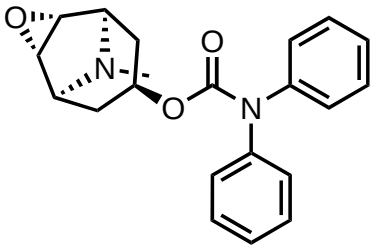

4 METHODS

4.1 CELL CULTURE

Cells were cultivated in incubators allowing growth at 37°C in a 5% CO_2 atmosphere. The medium used was F-12 Nutrient Mixture (Ham), which contains L-glutamine (1 mM) as an essential component. 10% fetal bovine serum (FBS) and 250 µg/ml geniticin were also added to this mixture.

4.1.1 SPLITTING ADHERENT CELLS

The transfected CHO cell lines grew exponentially and at around 80% confluency they had to be splitted, approximately twice a week. A microscope was used to check cell density and microbiological contamination.

The cell splitting procedure started under sterile conditions in the laminar air hood by removing the old medium from the flasks. Dulbecco's phosphate buffered saline (DPBS) was then pipetted into the flasks, to wash the cells, and then it was removed. Afterwards trypsin was added to the cells and incubation of the flask for five minutes followed. The presence of floating detached cells was checked under the microscope. The next step was to add new medium to the flasks, twice the amount of trypsin, then the cell - trypsin- medium mixture was removed. Finally, new medium was added, and the flasks were placed in the incubator to restore exponential grow.

4.1.2 FREEZING CELLS

For long time storage of the transfected CHO cell lines, the cells must be stored in a nitrogen tank. The first step was to place Mr. Frosty, a freezing box, in the freezer in advance. The freezing medium was prepared by adding 10% DMSO to the complete culture medium. After splitting the cells, the cells were resuspended with the freezing medium. A final concentration of transfected CHO cells of approximately $4x10^5$ was aimed for. The cell suspension was aliquoted into labelled cryotubes, each with a volume of 1.8 ml. Finally, the tubes containing the cells were placed in the -80°C freezer inside Mr. Frosty. After one day, the cells were transferred from Mr. Frosty into the nitrogen tank.

4.1.3 THAWING CELLS

Thawing the cells was needed before usage. The cells in cryovials were taken out of the -80 °C freezer. The content of the cryovial and cell medium (10 ml) was put into a centrifuge tube. The centrifugation process was operated at 1200 revolutions per minute (rpm) for 7 minutes. The supernatant was removed and the pellet was resuspended with fresh medium. The cells were pipetted into a flask with prepared fresh medium.

4.1.4 MEMBRANE PREPARATION

Membrane suspension preparations from the transfected CHO cells were essential for the competitive radioligand binding experiments. Ten T175 flasks with the respective cell line and an approximate cell confluency of 80-90% were prepared in a laminar air flow (LAF) (Figure 9). For the preparation of the cell membranes the following items were prepared: DPBS, buffer 1, buffer 2 and protease inhibitor (the content of a vial lyophilized powder was dissolved in 10 ml purified water) (Table 5). Everything was stored on ice until use.

Table 5: Content of buffer 1, buffer 2 and protease inhibitor is described in this table.

buffer 1	10 mM TRIS/HCl, 1 mM EDTA, pH 7.4
buffer 2	50 mM TRIS/HCl, pH 7.4
protease inhibitor	AEBSF 2 mM, Aprotinin 0.3 µM, Bestatin 116 µM, E-64 14 µM, Leupeptin 1 µM, EDTA 1 mM

The first step was to turn on the centrifuge and ultracentrifuge to achieve cooling of the devices to 4°C. The cells were taken from the incubator on ice. The old medium was removed from the cells, then they were washed with DPBS. The next step was to pipette 2 ml of buffer 1 and scrape the cells from the flasks. Then, these 2 ml of cell-buffer mixture were transferred to a 5 ml reagent tube that already contained 400 µl of protease inhibitor. After scraping the cells from all 10 flasks, each 5 ml reagent tube contained 400 µl of protease inhibitor plus the cell-buffer mixture from 2 flasks.

A syringe with G27 needle was used to transfer the mixture into the Potter Elvehjem homogenizer. With this device, the sample and buffer are forced through the cylindrical part of the mortar while the pestle rotates downward. This is a hand-held process that is repeated 10-15 times to achieve cell disruption. After breaking the cells, the mixture was returned to the 5 ml reagent tube. The first centrifugation was performed for 10 min at 1,000g and 4°C. In the next step, the pellet was removed, and the supernatant was transferred to ultracentrifuge tubes. The second centrifugation with ultracentrifuge lasted for 60 minutes at 10,000g and 4°C. Then the supernatant was removed, the pellet was taken out and resuspended with buffer 2. For each ultracentrifuge tube, 250 µl of buffer 2 was used. Finally, the membrane preparation suspensions obtained were aliquoted into cryovials. Each cryovial contained between 150 and 250 µl of membrane suspension, depending on the mAChR subtype of the cell lines used. For the M_1, M_3, and M_5 subtypes, 150 µl of membrane suspension was used, whereas 250 µl was required for the M_2 and M_4 experiments. The cryovials containing the membrane preparations were stored at -80°C in the freezer. The maximal time of storage due to decrease in the quality of these preparations, was 4-5 months.

Figure 9: A picture of the laminar airflow sterile cabinet, the workplace in the cell culture lab. Medical University of Vienna, Nuclear Medicine Department.

4.2 COMPETITIVE RADIOLIGAND BINDING ASSAY

4.2.1 EXPERIMENT PREPARATION

Three elements were essential for the competitive radioligand binding experiments: test ligands, the radiolabelled ligand and membrane preparations containing each mAChR subtype. DMSO was used to dilute the ligands (highest DMSO amount: 1%). Washing buffer and binding buffer, described in table 6, were prepared before starting the experiments and stored in the refrigerator.

Table 6: Content of washing buffer and binding buffer is described in this table.

washing buffer	50 mM TRIS, pH 7.4
binding buffer	10 mM $MgCl_2$, 1 mM EDTA, 50 mM TRIS, pH 7.4

Each experiment included two different test ligands. The first step was to prepare the dilution series for these ligands, since five different concentrations of the ligand were used for each experiment. The stock dilution had a 100 times higher concentration of the ligand than later in the experiment in the cell harvester tubes.

Table 7: Example of a dilution series for a test substance. The concentrations were adjusted for some of the compounds after the first experiment results.

Number	1.	2.	3.	4.	5.
concentration of stock solution	1 µM	10 µM	50 µM	100 µM	1 mM
concentration in harvester tube	10 nM	100 nM	500 nM	1 µM	10 µM

4.2.2 CELL HARVESTER

For one experiment, 36 cell harvester tubes were required. To ensure reproducibility, the experiment was conducted in three replicates and in three independent repetitions. The experiment started with pipetting, 5 µl DMSO/ cold scopolamine as reference compound/ test ligand into the tubes. The first three tubes contained DMSO, and the second three tubes contained scopolamine (100 µM in DMSO). For the test ligands, the lowest concentration was pipetted first, then the concentration was increased, followed by the second test ligand, as shown in table 8. In this table Sx represents test substance and Scop. represents cold scopolamine (100 µM in DMSO).

Table 8: Pipetting scheme for harvester tubes. 5 µl substance was pipetted in the tubes. Scop = scopolamine, S_x = test ligand with different concentrations.

S_2-2	S_2-2	S_2-2	S_2-3	S_2-3	S_2-3	S_2-3	S_2-4	S_2-4	S_2-5	S_2-5	S_2-5
S_1-3	S_1-3	S_1-3	S_1-4	S_1-4	S_1-4	S_1-5	S_1-5	S_1-5	S_2-1	S_2-1	S_2-1
DMSO	DMSO	DMSO	Scop.	Scop.	Scop.	S_1-1	S_1-1	S_1-1	S_1-2	S_1-2	S_1-2

After pipetting 5 µl substance into each tube 50 µl radioligand ([^{3}H] NMS) was added to all tubes. Different concentrations of the radioligand, depicted in table 9, were used depending on the mAChR subtype used in the experiment. The cells transfected with different subtypes have different expression rates. Before screenings, there were experiments performed with different concentrations of the radioligand for each subtype and a compromise between the amount of signal and used radioligand was found. The different K_D values of the radioligand against the different subtypes is the reason for using different concentrations of [^{3}H] NMS. In general, the higher the K_D to a subtype, the more radioligand must be used in order to get a sufficient amount of binding.

Table 9: The radioligand had a different concentration for each mAChR subtype. The dilutions were made by using binding buffer.

mACh receptor subtype	Concentration of [^{3}H] NMS
M_1	2 nM
M_2	3 nM
M_3	8 nM
M_4	2 nM
M_5	10 nM

Finally, the membrane preparation containing the desired mAChR subtype for the experiment was dissolved in binding buffer, so that 445 µl of membrane - buffer mixture was pipetted into each cell harvester tube to reach the volume of 500 µl. At this point, the tubes contained all the elements of the experiment, and the content had to be mixed using a vortex device. A reaction time of 1.5 hours at room temperature was required for the experiment.

After the 1.5 hour reaction period, the cell harvester, a laboratory device used to harvest biologics from tubes onto a glass fibre filter paper, was used (Figure 10). The GF/B filter had to be soaked with a 0.5% polyethyleneimine (PEI) solution for at least 10 minutes before filtration, to create a positive surface charge that helps trap negatively charged membrane fragments. Before and after using the cell harvester, the device had to be washed with cold washing buffer. After washing the device with washing buffer, the experiment was filtered with the harvester to separate the receptor bound ligands from the free ligands present in the mixture. After that the device was washed again with cold washing buffer. The GF/B filter paper containing the membrane fragments with the receptor bound ligands was then stamped out in a circular shape and placed into beta counting tubes.

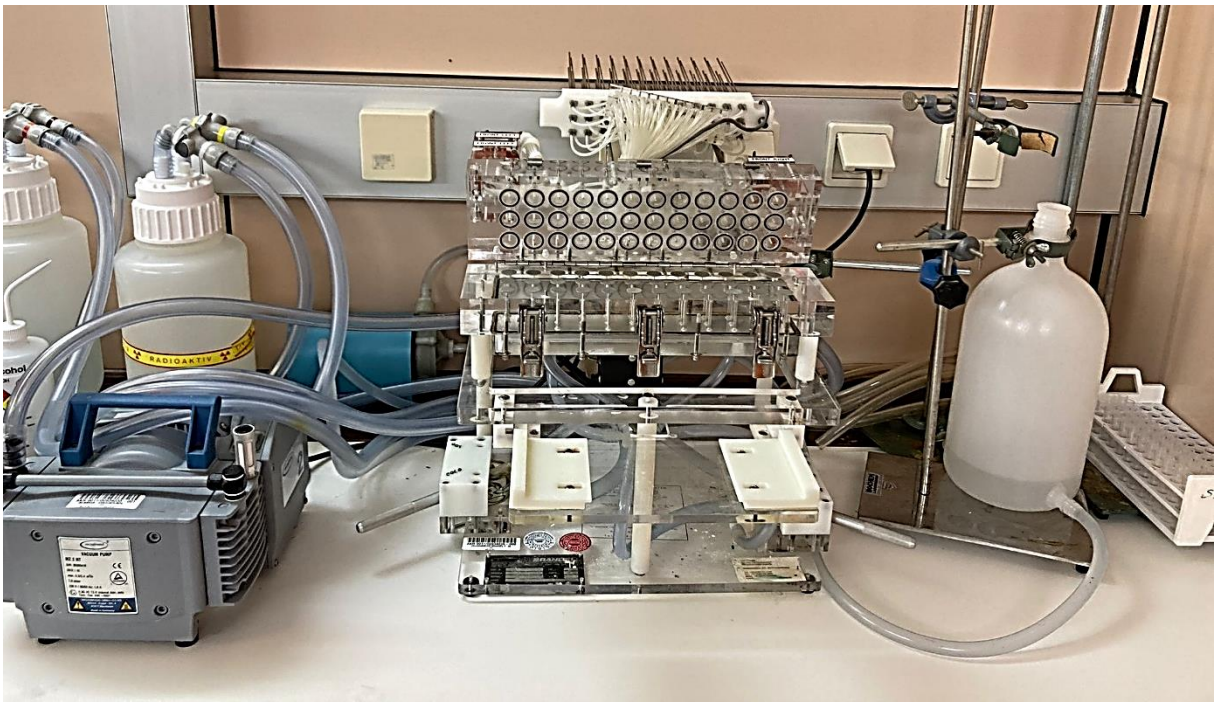

Figure 10: This picture shows the cell harvester (Brandel). Medical University of Vienna, Nuclear Medicine Department.

4.2.3 BETA COUNTER

2 ml of Ultima Gold ™ scintillation cocktail was added to the beta counter sample tubes containing the circular filter papers, as the beta radiation is not energetic enough to pass through the tube and cannot be detected by an external scintillator. After sealing the tubes, they were placed on a shaker for about ten minutes. Finally, the tubes were placed in the beta counter. (Figure 11) The liquid scintillation cocktail converted the kinetic energy of the nuclear emission into UV light. The light passed through the sample container and was translated into a measure of the radioactivity of the sample. At the end of the measurement, the results were converted to an excel file. Generally, the measurements with pure DMSO have the highest radioactivity and CPM (counts per minute) values as there is no competition between DMSO and [^{3}H] NMS for the receptor. Scopolamine (100 µM in DMSO) measurements have the least amount of radioactivity and the lowest CPM values because of the competition between cold and hot scopolamine. The results of the test compounds have CPM values in between.

The CPM values were entered into the GraphPad Prism program and were plotted against the logarithms of the concentrations of the test compounds used. With GraphPad Prism the nonlinear regression (curve fit) and log (inhibitor) vs response – variable slope parameters were used, and the program generated the inhibition curves. In the program the table of results show important calculated values of the experiments, for example the determined IC_{50} value. The K_i values were calculated using the Cheng-Prusoff equation with the IC_{50} values determined and K_D values of [^{3}H] NMS from literature described in table 3.

Figure 11: The Hidex 300 SL beta radiation counter is shown with the sample tubes already placed in the instrument. Medical University of Vienna, Nuclear Medicine Department.

RESULTS AND DISCUSSION

The binding properties of all sixteen test ligands towards the five mAChR subtypes were determined by competitive radioligand binding experiments and calculations using the Cheng-Prusoff equation were performed. Screenings were made with the compounds in order to determine if the ligands have binding affinity in a range required for PET tracers, and so can be moved forward to the radioligand binding experiments for evaluation of the exact K_i values. For efficient binding affinity the K_i value of a ligand should be in the low nanomolar range. If a compound had K_i > 1000 nM for an individual subtype in the screening process the subtype was excluded from experiments as it was out of the range of our interest. In these cases, test ligands were only tested towards the subtypes where they exhibited sufficiently good binding properties in screenings. Twelve ligands were profiled against all five subtypes of the receptor at several different concentrations and four compounds had individual experimenting plans. (Table 10).

Table 10: This table describes which receptor subtypes were used with the test ligands.

Tested subtype	Compound
M_1 - M_5	ARA 35, ARA 54, ARA 55, ARA 56, ARA 117, ARA 122, ARA 154, ARA 156, ARA 166, MIMA 195, RR 41, RR 43
M_1 - M_4	MIMA 174
M_1, M_3, M_4, M_5	RR 37 and RR 39
M_3, M_4	RR 40

ARA 35, ARA 54, ARA 55, ARA 56, ARA 117, ARA 122, ARA 154, ARA 156, ARA 166, MIMA 195, RR 41 and RR 43 were tested with all five receptor subtypes. For four test substances, RR 37, RR 39, RR 40, MIMA 174, individual receptor subtypes did not need to be experimented on, as these compounds did not have K_i values <1000 nM as evaluated in previous screenings towards specific subtypes. Experiments were not performed with MIMA 174 on the M_5 subtype. For RR 37 and RR 39 the M_2 subtype did not need to be profiled. RR 40 was only applied with the M_3 and M_4 receptor subtypes.

For radiotracer development excellent binding affinity with inhibition constant value in the low nanomolar range is essential. For the results we defined specific target K_i values. We defined our own standards for identification of the most potent compounds. Thereby, we defined an excellent binding affinity of a test ligand with a K_i value in the low nanomolar range of <10 nM. Inhibition constant value between 10 nM and 50 nM indicates good binding affinity while >50 nM K_i implies low affinity of the test ligand towards the mAChR. The subtype selectivity between the receptor subtypes can be described with the ratio of the K_i values to one another. The bigger the difference in the inhibition constant values the better the subtype selectivity. We also defined target values for the subtype selectivity. A ratio <10 implies no subtype selectivity while the ratio being >10 stands for intermediate selectivity of the test ligand. A ratio >50 signifies excellent receptor subtype selectivity.

The most promising compounds in regards of the receptor binding affinity of the compounds is depicted in table 11.

Table 11: This table summarizes the compounds with the best inhibition constant values for each mAChR subtype.

	M_1	M_2	M_3	M_4	M_5
excellent binding affinity K_i < 10 nM	ARA 54 ARA 55	-	-	ARA 54	ARA 54 ARA 55
good binding affinity 10 nM < K_i < 50 nM	ARA 35 ARA 56 ARA 122 ARA 156 RR 41	ARA 54	ARA 54 ARA 55 MIMA 174	ARA 55 ARA 56 RR 41	ARA 56

The results revealed excellent binding affinity profile for compounds ARA 54 and ARA 55 for the M_1 receptor. Good binding affinity was achieved with test ligands ARA 35, ARA 56, ARA 122, ARA 156 and RR 41 for the M_1 subtype. The only important compound for M_2 receptor binding was the test ligand ARA 54. Good binding properties for the M_3 subtype had ARA 54, ARA 55 and MIMA 174. MIMA 174 is the only compound that favours the M_3 receptor, all the other compounds have the best results with the M_1 receptor subtype.

Compound ARA 54 showed excellent affinity for the M_4 receptor subtype while ARA 55, ARA 56 and RR 41 had good affinity results for this receptor. ARA 54 and ARA 55 exhibited excellent binding affinity values for the M_5 subtype and ARA 56 showed good affinity for this receptor subtype.

The least promising compounds were ARA 117, ARA 154, MIMA 195, RR 37, RR 39, RR 40, RR 43. All of these test ligands had only low binding affinities > 50 nM K_i with all of the subtypes. Seven compounds had K_i values above the cut off value of 1000 nM towards individual subtypes in the experiments (Table 12). This cut off value was defined as for PET radiotracer development a nanomolar affinity of the compound is required.

Table 12: Compounds with very low binding affinity to individual subtypes are described in this table.

	M_1	M_2	M_3	M_4	M_5
very low binding affinity K_i >1000 nM	RR 43	ARA 35 ARA 117 ARA 122 ARA 156 MIMA 195 RR 43	ARA 154 RR 43	RR 43	RR 43

ARA 35, ARA 117, ARA 122, ARA 156, MIMA 195 and RR 43 all had very low binding properties with the subtype M_2. Above the cut off K_i value for the M_3 subtype measured ARA 154 and RR 43. RR 43 was the only compound that had K_i results above the cut off value for all five receptor subtypes.

As mentioned before to ensure reproducibility, to every experiment three independent repetitions were completed. There were exceptions to that, if in the first or first two experiments the results showed K_i values above 1000 nM further experiments were not performed (n= 1/2) as so the compounds were out of the range of interest.

Compound ARA 35 showed the highest binding affinity towards the M_1 receptor subtype with a K_i value measured 15 ± 4 nM followed by similarly good binding properties against M_4 and M_5 with K_i values at 55 ± 21 nM and 51 ± 4 nM. The affinity decreased for the subtype M_3 with an inhibition constant value evaluated at 226 ± 85 nM. ARA 35 showed the lowest affinity for the M_2 subtype with a K_i value above the 1000 nM cut off value: 2411 ± 1002 nM. The 160-fold subtype selectivity of compound ARA 35 to the M_1 receptor in opposite to the M_2 subtype is excellent. The K_i ratio between M_1 and M_3 is >15 so the selectivity to M_1 is intermediate. There is no significant difference in the K_i values between M_1, M_4 and M_5 which indicates no subtype selectivity towards M_1 in opposition to these receptors.

ARA 54 had promising binding properties for all subtypes. The best binding affinity was measured for the M_1 subtype with a K_i value of 1.22 ± 0.06 nM. The affinity decreased in the order from $M_1 > M_5 > M_4 > M_3 > M_2$. The inhibition constant value determined for M_5 was 4 ± 1 nM for M_4 6 ± 2 nM and for M_3 it was 16 ± 5 nM. The lowest affinity for compound ARA 54 was achieved with the M_2 receptor, where the inhibition value was measured at 33 ± 11 nM. The K_i ratio between M_1 and both M_2 and M_3 were >10 but <50 which implies an intermediate subtype selectivity to the M_1 receptor subtype. There is no subtype selectivity for ARA 54 towards M_1 in opposition to the M_4 and M_5 receptors.

Test ligand ARA 55 showed excellent binding affinity against the M_1 subtype with a K_i value of 1.2 ± 0.4 nM. The lowest affinity with an inhibition constant of 227 ± 86 nM was measured for the M_2 subtype. The inhibition constant values determined of the other subtypes were 5 ± 2 nM for M_5, 14 ± 6 nM for M_4 and 28 ± 11 nM for the M_3 subtype. The receptor subtype selectivity for M_1 in opposition to M_2 was excellent for ARA 55. M_1 selectivity was intermediate against the M_3 and M_4 receptors. The K_i value difference between M_1 and M_5 was <10 which implies low selectivity for M_1.

ARA 56 had comparable binding properties to M_1 and M_4 with K_i values evaluated at 17 ± 3 nM for M_1 and 20 ± 6 nM for M_4. The affinity to the subtype M_5 was good with a K_i value of 42 ± 15 nM. The lowest affinity according to the results with compound ARA 56 was determined towards the M_2 and M_3 receptors with inhibition constant values at 850 ± 40 nM and 142 ± 24 nM, respectively. This test ligand showed excellent subtype selectivity for the M_1 receptor in opposition to the M_2 subtype. The differences in K_i values between the M_1, M_3, M_4 and M_5 receptors was not convincing enough to indicate good selectivity for the M_1 receptor subtype.

Compound ARA 117 had similar low affinities to all subtypes except the M_2 receptor. The inhibition constant value was 239 ± 68 nM for M_1, 277 ± 45 nM for M_3, 238 ± 104 nM for M_4 and 295 ± 33 nM for the M_5 receptor subtype. ARA 117 tested above the cut off value of 1000 nM for the M_2 subtype with a K_i value of 1480 ± 972 nM. The ratio between the K_i values of all five mAChR subtypes imply no selectivity of this compound towards the M_1 receptor subtype.

ARA 122 showed good binding affinity with a K_i value of 25 ± 6 nM for the M_1 receptor subtype. This compound demonstrated low binding properties to the other subtypes. The inhibition constant values were comparable for M_3 and M_4 at 165 ± 38 nM and 151 ± 53 nM, respectively. The affinity of the test ligand ARA 122 decreased for the M_5 subtype with a K_i value of 231 ± 26 nM. The inhibition constant for the M_2 receptor subtype was measured to be above the cut of value of 1000 nM, with a value of 9030 ± 4203 nM. The results signify that this test ligand has no relevant selectivity for M_1 towards the M_3, M_4 and M_5 receptor subtypes. The only compelling difference in the K_i values was calculated between M_1 and M_2 which suggests high selectivity for the M_1 receptor.

Test ligand ARA 154 showed similarly low affinities with most of the mAChR subtypes. The best K_i value of 475 ± 89 nM was found for the M_1 receptor. Inhibition constant value of 521 ± 173 nM was measured for subtype M_5, 563 ± 73 nM for M_4 and 624 ± 104 nM for M_2, respectively. Experiment results showed the lowest binding affinity towards the M_3 receptor with a K_i value just slightly above the cut off value of 1000 nM, 1063 nM (n=1). The comparison of the K_i values implies that compound ARA 154 has no selectivity to any mAChR subtype.

Good binding affinity was achieved using compound ARA 156 with the subtype M_1. The K_i value was 33 ± 8 nM. The inhibition constant values increase in the order of M_1 > M_5 > M_4 > M_3 > M_2. The K_i values were 68 ± 22 nM for M_5, 115 ± 51 nM for M_4 and 358 ± 83 nM for M_3. The inhibition constant value of this test ligand towards the M_2 receptor subtype was evaluated 1505 ± 108 nM (n=2), which is above the cut off value of 1000 nM. The difference in the K_i values between the M_1 and the other subtypes demonstrate that ARA 156 has an intermediate selectivity for M_1 in opposition to M_2 and M_3. The results show no subtype selectivity for the M_1 receptor against the other two subtypes.

The compound ARA 166 had an intermediate affinity to the M_1 and M_5 mAChR subtypes with inhibition constant values of 68 ± 5 nM for M_1 and 65 ± 23 nM for M_5. Similar K_i values were calculated for the M_3 and M_4 subtypes with values of 181 ± 68 nM for M_3 and 144 ± 37 nM for M_4. The lowest binding affinity was measured for the M_2 receptor with a K_i value of 722 ± 101 nM. This test ligand had no selectivity for M_1 against the $M_{3/4/5}$ receptor subtypes according to the calculated K_i values and their comparison to one another. An intermediate subtype selectivity was only found for M_1 vs. M_2 receptor of 11-fold increased affinity towards the M_1 subtype.

MIMA 174 had a good binding affinity for the subtype M_3 with a K_i value of 46 ± 11 nM. The inhibition constant value for M_1 was 101 ± 39 nM, 201 ± 65 nM for M_4 and 443 ± 150 nM for M_2. Competitive radioligand binding experiment was not performed with MIMA 174 on the M_5 receptor subtype, as the compound showed no K_i values in nanomolar range in previous screenings. The differences in the K_i values to the receptor subtypes are not pronounced enough to demonstrate subtype selectivity.

Compound MIMA 195 showed similar binding affinity for the M_4 and M_5 subtypes with K_i values of 189 ± 57 nM for M_4 and 164 ± 43 nM for M_5. The affinity decreased in the order M_5 > M_4 > M_1 > M_3 > M_2 with inhibition constant values of 285 ± 16 nM for M_1 and 350 ± 120 nM for M_3. The compound MIMA 195 had a K_i above the cut off value 1000 nM for the M_2 receptor subtype 4476 ±2968 nM. The comparison of the inhibition constant values shows a low subtype selectivity of this test ligand to either of the mACh receptor subtypes.

There was no competitive radioligand binding experiment performed with RR 37 towards the M_2 subtype due to the insufficient affinity as evaluated in previous screenings. The inhibition constants of RR 37 to the other four receptor subtypes resulted in comparable values. The order of ligand affinity is as follows: $M_5 > M_3 > M_4 > M_1$. The K_i value was calculated 105 ± 6 nM for M_5, 123 ± 19 nM for M_3, 156 ± 28 nM for M_4 and 217 ± 22 nM for the M_1 subtype. Based on these results no convincing selectivity was expressed by the compound RR 37.

The binding affinity of ligand RR 39 for the receptor subtype M_2 was not in the required range for the development of PET tracers. The highest affinity was demonstrated with the M_3 subtype with a K_i value of 121 ± 40 nM. The compound RR 39 had an inhibition constant value of 158 ± 34 nM for the M_4 receptor, 255 ± 7 nM for the M_1 and 255 ± 41 nM for the M_5 receptor subtype. The results indicate that no relevant subtype selectivity was found for RR 39.

The screenings for RR 40 resulted in the exclusion of the M_1, M_2 and M_5 receptors from the competitive radioligand binding experiments, due to the low affinity of the compound towards these receptors. The inhibition constant value of RR 40 of the M_4 subtype was 244 ± 92 nM and of the M_3 subtype 339 ± 33 nM.

The compound RR 41 demonstrated similar good binding affinity to both the M_1 and the M_4 receptor. The K_i value was 44 ± 2 nM for the M_1 subtype and 50 ± 20 nM for the M_4 subtype. The inhibition constant value belonging to the M_5 receptor was 75 ± 35 nM. Higher K_i values were measured for the last two receptor subtypes, namely 108 ± 31 nM for M_3 and 222 ± 49 nM for M_2, respectively. Also, RR 41 showed no relevant subtype selectivity.

Performed radioligand binding experiments resulted in inhibition constant values highly above the cut off value of 1000 nM, with all five receptor subtypes using the compound RR 43.

Table 13: This table shows the K_i values of the 16 test compounds towards the five different mAChR subtypes representing the binding affinity, along with the ratio between the K_i values of the test ligands with the M_1 receptor subtype and the other subtypes to evaluate selectivity.

Compound	K_i [nM]					Ratio			
	M_1	M_2	M_3	M_4	M_5	$\frac{M_2}{M_1}$	$\frac{M_3}{M_1}$	$\frac{M_4}{M_1}$	$\frac{M_5}{M_1}$
ARA 35	15 ± 4	>1000	226 ± 85	55 ± 21	51 ± 4	>66	15	3.7	3.4
ARA 54	1.22 ± 0.06	33 ± 11	16 ± 4	6 ± 2	4 ± 1	27	13	4.9	3.3
ARA 55	1.2 ± 0.4	227 ± 86	28 ± 11	14 ± 6	5 ± 2	189	23	12	4,2
ARA 56	17 ± 3	850 ± 40	142 ± 24	20 ± 6	42 ± 15	50	8,4	1.2	2.5
ARA 117	239 ± 68	>1000	277 ± 45	238 ± 104	295 ± 33	4.2	1.2	0.99	1.2
ARA 122	25 ± 6	>1000	165 ± 38	151 ± 53	231 ± 26	40	6.6	6.0	9.2
ARA 154	475 ± 89	624 ± 104	>1000	563 ± 73	521 ± 172	1.3	2.1	1.2	1.1
ARA 156	33 ± 8	>1000	358 ± 83	115 ± 51	68 ± 22	30	11	3.5	2.1
ARA 166	68 ± 5	722 ± 101	181 ± 68	144 ± 37	65 ± 23	11	2.7	2.1	0.99
MIMA 174	101 ± 39	443 ± 150	46 ± 11	201 ± 65	-	4.4	0.5	2.0	-
MIMA 195	285 ± 16	>1000	350 ± 120	189 ± 57	164 ± 43	1.2	3.5	0.7	0.6
RR 37	217 ± 22	-	123 ± 19	156 ± 28	105 ± 6	-	0.6	0.7	0.5
RR 39	255 ± 7	-	121 ± 40	158 ± 34	255 ± 41	-	0.5	0.6	1.0
RR 40	-	-	339 ± 33	244 ± 92	-	-	-	-	-
RR 41	44 ± 2	222 ± 49	108 ± 31	50 ± 20	75 ± 35	5.0	2.5	1.1	1.7
RR 43	>1000	>1000	>1000	>1000	>1000	-	-	-	-

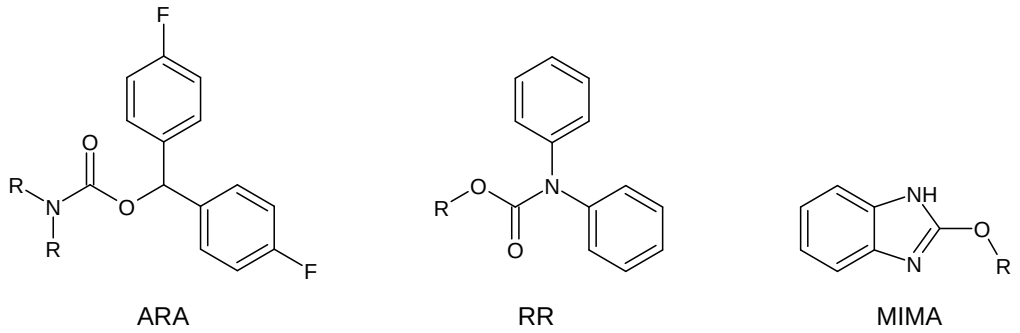

Figure 12: Comparison of the structures of ARA, RR and MIMA. The rest includes the methyl-amine motif relevant for binding to the orthosteric binding site of the mAChR.

All ARA compounds are furnished with a 4,4'-difluorobenzhydrol carbamate moiety further connected to a cyclic amine bearing a methylated amine (Figure 12). The RR compounds are structurally related to the ARA ones; however, the two phenyl groups are bound to the nitrogen of the carbamate linker. Two MIMA test ligands were further tested in the radioligand binding experiments. These compounds have a benzimidazole bound to the required cyclic amine motif. This structural feature was adjusted from a recently found rearrangement product of pirenzepine, a very well-established parasympatholytic drug.[42] It was shown in previous publications, that the methylated cycloamine motif is essential for the binding to mAChRs.[43,44,45] As seen in table 14, the ARA, RR and MIMA compounds were furnished with different 4, 5, 6 and 7-membered rings.

In overall, all ARA based compounds show a higher affinity than the RR and MIMA based compounds.

Table 14: Secondary and tertiary amine binding motif.

ARA	RR	MIMA
4-membered rings		
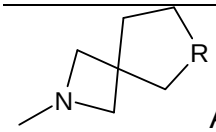 ARA 122	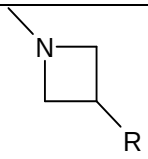 RR 37	
5-membered rings		
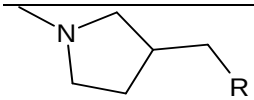 ARA 117		
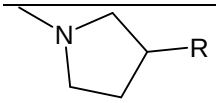 ARA 166	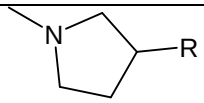 RR 39	
6-membered rings		
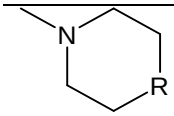 ARA 35	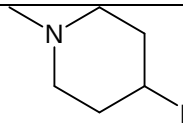 RR 40	
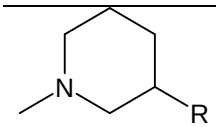 ARA 54		
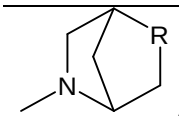 ARA 156		

7-membered rings

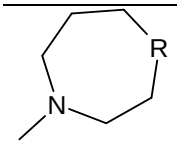

ARA 55

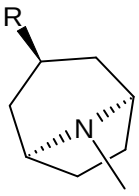

RR 41

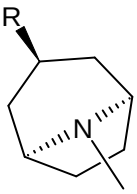

MIMA 174

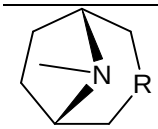

ARA 56

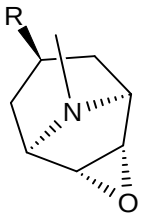

RR 43

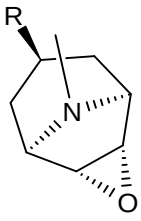

MIMA 195

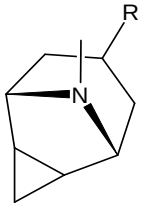

ARA 154

The most affine compounds were found in the groups of the 6 or 7 membered rings, whereas the 4 and 5-membered ones were generally less affine.

Comparing ARA 54 and ARA 55, both compounds have affinities for M_1 in the range of 1 nM, have the same chemical formula and consequently the same molecular weight. Structural differences were only at the cycloamine motif, with ARA 54 having a 6-membered ring with the carbamate being not included in the ring system, whereas ARA 55 includes the carbamate into the 7-membered ring. However, including the carbamate into the 6-membered ring, as seen for ARA 35, reduces the activity again. Changing the 6- to a 5-memebered ring further reduces the affinity, as seen for ARA 166. Addition of a methylene spacer between the 5-membered ring and the carbamate further reduces the affinity and excludes ARA 117 from further evaluations.

Introduction of any additional amine bridges into any compound, reduces the affinity and is therefore not preferred.

The clogP value of a ligand targeting the CNS the BBB penetration is an essential criterion. Pajouhesh at al defines an optimal range of clogP values for central nervous system drugs in the range of 1.5-2.7, with the mean value of 2.1.[41] The tested compounds have a clogP range of 1.12-4.10, which means that 63% of the here tested compounds are out of the optimal range. On the other hand, Lipinski's rule of five describes a target clogP < 5. In this case 100% of our test compounds are in the optimal range. [46]

Correlation between the clogP value of the tested compounds and the K_i value results for the M_1 receptor subtype was analysed. (Table 15, Figure 13). The data in table 15 is lined up according to the increasing clogP values.

Table 15: This table shows the clogP and K_i values for the M_1 subtype of the sixteen tested compounds to analyse correlation between the two values.

Compound name	clogP	K_i [nM]
ARA 117	1.12	239
ARA 156	1.37	33
ARA 166	1.77	68
ARA 56	1.92	17
ARA 122	2.08	25
ARA 154	2.31	475
ARA 54	2.44	1.22
MIMA 195	2.69	285
RR 40	3.01	1000
RR 37	3.10	217
ARA 35	3.14	15
ARA 55	3.19	1.2
MIMA 174	3.78	101
RR 39	3.78	255
RR 43	4.01	1000
RR 41	4.10	44

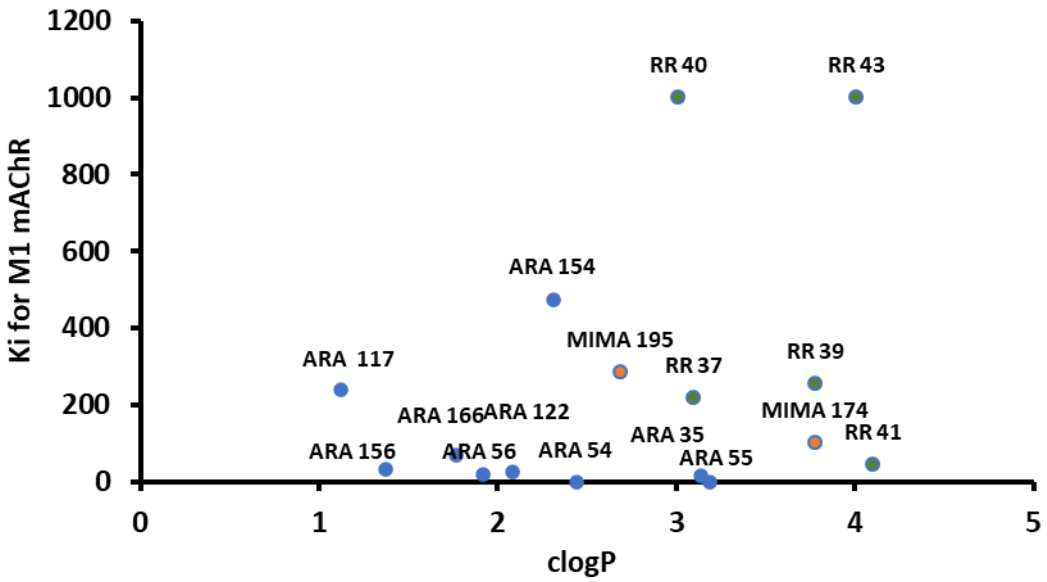

Figure 13: This figure shows that there is no correlation between the clogP and the K_i values. The x-axis presents the increasing clogP values while the y-axis presents the K_i values belonging to them.

As expected, no linear correlation was found between the K_i and the clogP values. Interestingly, the best binding affinity results are located in the lower clog P region between 1.37 and 2.44, with the exception of 2.31. Excellent M_1 receptor binding affinity is also present between clogP 3.14 and 3.78.

For PET radiotracer development binding affinity, selectivity profile and the clogP value of the compound are important. The most suitable ligands for further development due to their desirable parameters out of all sixteen compounds tested are the compounds ARA 54 and ARA 55. They both have the 4,4'-difluorobenzhydrol carbamate structure that is connected to a 6/7 membered cyclic amine ring.

CONCLUSION

The binding properties of sixteen newly synthesized potential mAChR antagonists was investigated in competitive radioligand binding experiments and K_i values calculated using the Cheng-Prusoff equation for all five receptor subtypes of the mAChR. Our goal was to identify the most potent compounds with a high subtype selectivity and to draw structure-activity relationships to improve the next series of compounds.

The most promising compounds, ARA 54 and ARA 55, showed a high affinity in the low nanomolar range for M_1, M_4 and M_5 receptors. ARA 55 outperformed ARA 54 in terms of subtype selectivity. In general, the ARA compounds were more potent compared to the RR and MIMA compounds. RR 41 had the highest affinity out of the RR group with good binding affinity towards subtypes M_1 and M_4. Compound MIMA 174 was superior to MIMA compound 195. MIMA 174 is the only test ligand, which had a preference for the M_3 subtype, whereas all the other compounds favoured the M_1 receptor.

In regards of the selectivity of the compounds for the M_1 receptor subtype the results are not that promising. The best selectivity results are presented in comparison with the M_2 receptor for most of the compounds. This outcome further demonstrates the difficulty of developing subtype selective mAChR orthosteric antagonists.

The structure-activity relationships implied that 6- or 7-membered binding motifs are better fitting to the binding pocket of the mAChRs, whereas 4- or 5-membered rings are less preferred. Introduction of an amine-bridge into the cycloamines reduced the affinity of the compounds significantly. Correlation between the clogP value of the tested compounds and the K_i value results for the M_1 receptor subtype was analysed and no significant correlation could be demonstrated.

In conclusion, ARA 55 is the compound of choice for further evaluation towards the establishment of a potential mAChR PET tracer.

TABLE OF TABLES

TABLE OF FIGURES

TABLE OF EQUATIONS

Equation 1: This equation describes receptor-ligand binding interaction. R: unbound receptor, L: free ligand, k_{on}: association constant, k_{off} dissociation constant RL: receptor-ligand complex.

Equation 2: This equation describes the equilibrium association constant K_a. RL: receptor-ligand complex, R: unbound receptor, L: free ligand, k_{on}: association constant, k_{off} dissociation constant, K_a: equilibrium association constant.

Equation 3: The equation describes the equilibrium dissociation constant K_D. R: unbound receptor, L: free ligand, RL: receptor-ligand complex, k_{off} dissociation constant, k_{on}: association constant, K_D: equilibrium dissociation constant.

Equation 4: The Cheng-Prusoff equation defines the relation between the K_i and the IC_{50} of an inhibitory ligand. K_i: inhibitor constant, IC_{50}: half-maximal inhibitory concentration, L: inhibitory ligand, K_D: equilibrium dissociation constant of the radioligand.

REFERENCES

1 Latorraca NR, Venkatakrishnan AJ, Dror RO. GPCR Dynamics: Structures in Motion. Chem Rev. 2017 Jan 11;117(1):139-155. doi: 10.1021/acs.chemrev.6b00177. Epub 2016 Sep 13. PMID: 27622975.

2 Hilger D, Masureel M, Kobilka BK. Structure and dynamics of GPCR signaling complexes. Nat Struct Mol Biol. 2018;25(1):4-12. doi:10.1038/s41594-017-0011-7

3 Lynch, J.R.; Wang, J.Y. G Protein-Coupled Receptor Signaling in Stem Cells and Cancer. Int. J. Mol. Sci. 2016, 17, 707. https://doi.org/10.3390/ijms17050707

4 Congreve M, de Graaf C, Swain NA, Tate CG. Impact of GPCR Structures on Drug Discovery. Cell. 2020 Apr 2;181(1):81-91. doi: 10.1016/j.cell.2020.03.003. PMID: 32243800.

5 Eichel K, von Zastrow M. Subcellular Organization of GPCR Signaling. Trends Pharmacol Sci. 2018;39(2):200-208. doi:10.1016/j.tips.2017.11.009

6 Fryer AD, Jacoby DB. Muscarinic receptors and control of airway smooth muscle. Am J Respir Crit Care Med. 1998 Nov;158(5 Pt 3):S154-60. doi: 10.1164/ajrccm.158.supplement_2.13tac120. PMID: 9817739.

7 Greig, N. H., Reale, M., & Tata, A. M. (2013). New pharmacological approaches to the cholinergic system: an overview on muscarinic receptor ligands and cholinesterase inhibitors. Recent patents on CNS drug discovery, 8(2), 123–141. https://doi.org/10.2174/1574889811308020003

8 Kruse AC, Kobilka BK, Gautam D, Sexton PM, Christopoulos A, Wess J. Muscarinic acetylcholine receptors: novel opportunities for drug development. Nat Rev Drug Discov. 2014 Jul;13(7):549-60. doi: 10.1038/nrd4295. Epub 2014 Jun 6. PMID: 24903776; PMCID: PMC5818261.

9 Randáková A, Jakubík J. Functionally selective and biased agonists of muscarinic receptors. Pharmacol Res. 2021 Jul;169:105641. doi: 10.1016/j.phrs.2021.105641. Epub 2021 May 2. PMID: 33951507.

10 Caulfield MP and Birdsall NJ (1998) International Union of Pharmacology. XVII. Classification of muscarinic acetylcholine receptors. Pharmacol Rev 50:279–290.

11 Kohnen-Johannsen KL, Kayser O. Tropane Alkaloids: Chemistry, Pharmacology, Biosynthesis and Production. Molecules. 2019;24(4):796. Published 2019 Feb 22. doi:10.3390/molecules24040796

12 Ozenil, M., Aronow, J., Millard, M., Langer, T., Wadsak, W., Hacker, M., & Pichler, V. (2021). Update on PET Tracer Development for Muscarinic

Acetylcholine Receptors. Pharmaceuticals (Basel, Switzerland), 14(6), 530. https://doi.org/10.3390/ph14060530

13 Felder, C.C. (1995), Muscarinic acetylcholine receptors: signal transduction through multiple effectors. The FASEB Journal, 9: 619-625. https://doi.org/10.1096/fasebj.9.8.7768353

14 Suridjan, I., Comley, R.A. & Rabiner, E.A. The application of positron emission tomography (PET) imaging in CNS drug development. Brain Imaging and Behavior 13, 354–365 (2019). https://doi.org/10.1007/s11682-018-9967-0

15 Kapoor M, Kasi A. PET Scanning. 2021 Oct 9. In: StatPearls [Internet]. Treasure Island (FL): StatPearls Publishing; 2022 Jan–. PMID: 32644515.

16 Berti V, Pupi A, Mosconi L. PET/CT in diagnosis of dementia. Ann N Y Acad Sci. 2011 Jun;1228:81-92. doi: 10.1111/j.1749-6632.2011.06015.x. PMID: 21718326; PMCID: PMC3692287.

17 Schwaiger M, Wester HJ. How many PET tracers do we need? J Nucl Med. 2011 Dec;52 Suppl 2:36S-41S. doi: 10.2967/jnumed.110.085738. PMID: 22144553.

18 Pichler V, Berroterán-Infante N, Philippe C, Vraka C, Klebermass EM, Balber T, Pfaff S, Nics L, Mitterhauser M, Wadsak W. An Overview of PET Radiochemistry, Part 1: The Covalent Labels 18F, 11C, and 13N. J Nucl Med. 2018 Sep;59(9):1350-1354. doi: 10.2967/jnumed.117.190793. Epub 2018 Jul 24. PMID: 30042159.

19 Naganawa, M., Nabulsi, N., Henry, S., Matuskey, D., Lin, S. F., Slieker, L., Schwarz, A. J., Kant, N., Jesudason, C., Ruley, K., Navarro, A., Gao, H., Ropchan, J., Labaree, D., Carson, R. E., & Huang, Y. (2021). First-in-Human Assessment of 11C-LSN3172176, an M1 Muscarinic Acetylcholine Receptor PET Radiotracer. Journal of nuclear medicine : official publication, Society of Nuclear Medicine, 62(4), 553–560. https://doi.org/10.2967/jnumed.120.246967

20 Mohammadi-Nejad, Ali-Reza & Mahmoudzadeh, Mahdi & Hassanpour, Mahlegha & Wallois, Fabrice & Muzik, Otto & Papadelis, Christos & Hansen, Anne & Soltanian-Zadeh, Hamid & Gelovani, Juri & Nasiriavanaki, Mohammadreza. (2018). Neonatal brain resting-state functional connectivity imaging modalities. Photoacoustics. 10. 10.1016/j.pacs.2018.01.003.

21 Lever SZ, Fan KH, Lever JR. Tactics for preclinical validation of receptor-binding radiotracers. Nucl Med Biol. 2017;44:4-30. doi:10.1016/j.nucmedbio.2016.08.015

22 Guo D, Peletier LA, Bridge L, et al. A two-state model for the kinetics of competitive radioligand binding. Br J Pharmacol. 2018;175(10):1719-1730. doi:10.1111/bph.14184

23 Shim J, Hong ZY, Sohn I, Hwang C. Prediction of drug-target binding affinity using similarity-based convolutional neural network. Sci Rep. 2021;11(1):4416. Published 2021 Feb 24. doi:10.1038/s41598-021-83679-y

24 de Jong LA, Uges DR, Franke JP, Bischoff R. Receptor-ligand binding assays: technologies and applications. J Chromatogr B Analyt Technol Biomed Life Sci. 2005 Dec 27;829(1-2):1-25. doi: 10.1016/j.jchromb.2005.10.002. Epub 2005 Oct 25. PMID: 16253574.

25 Hulme EC, Trevethick MA. Ligand binding assays at equilibrium: validation and interpretation. Br J Pharmacol. 2010;161(6):1219-1237. doi:10.1111/j.1476-5381.2009.00604.x

26 Hunter SA, Cochran JR. Cell-Binding Assays for Determining the Affinity of Protein-Protein Interactions: Technologies and Considerations. Methods Enzymol. 2016;580:21-44. doi:10.1016/bs.mie.2016.05.002

27 Kuraoka S, Ito Y, Wakuda H, Shinozuka K, Onoue S, Yamada S. Characterization of muscarinic receptor binding by the novel radioligand, [(3)H]imidafenacin, in the bladder and other tissues of rats. J Pharmacol Sci. 2016 Jul;131(3):184-9. doi: 10.1016/j.jphs.2016.06.002. Epub 2016 Jun 23. PMID: 27430986.

28 Sharma, Sai Kiran et al. “A rapid bead-based radioligand binding assay for the determination of target-binding fraction and quality control of radiopharmaceuticals.” Nuclear medicine and biology vol. 71 (2019): 32-38. doi:10.1016/j.nucmedbio.2019.04.005

29 National Center for Biotechnology Information (2022). PubChem Compound Summary for CID 16757568, [3H]-N-Methylscopolamine. Retrieved March 30, 2022 from https://pubchem.ncbi.nlm.nih.gov/compound/3H_-N-Methylscopolamine.

30 Hellmuth A., Calderón Villalobos L.I.A. (2016) Radioligand Binding Assays for Determining Dissociation Constants of Phytohormone Receptors. In: Lois L., Matthiesen R. (eds) Plant Proteostasis. Methods in Molecular Biology, vol 1450. Humana Press, New York, NY. https://doi.org/10.1007/978-1-4939-3759-2_3

31 Hoare SRJ. Analyzing Kinetic Binding Data. 2021 Apr 1. In: Markossian S, Grossman A, Brimacombe K, Arkin M, Auld D, Austin CP, Baell J, Chung TDY, Coussens NP, Dahlin JL, Devanarayan V, Foley TL, Glicksman M, Hall MD, Haas JV, Hoare SRJ, Inglese J, Iversen PW, Kales SC, Lal-Nag M, Li Z, McGee J, McManus O, Riss T, Saradjian P, Sittampalam GS, Tarselli M, Trask OJ Jr, Wang Y, Weidner JR, Wildey MJ, Wilson K, Xia M, Xu X, editors. Assay Guidance Manual [Internet]. Bethesda (MD): Eli Lilly & Company and the National Center for Advancing Translational Sciences; 2004–. PMID: 33852262.

32 Pollard TD. A guide to simple and informative binding assays. Mol Biol Cell. 2010 Dec;21(23):4061-7. doi: 10.1091/mbc.E10-08-0683. PMID: 21115850; PMCID: PMC2993736.

33 Casadó-Anguera, V., Moreno, E., Mallol, J., Ferré, S., Canela, E. I., Cortés, A., & Casadó, V. (2019). Reinterpreting anomalous competitive binding experiments within G protein-coupled receptor homodimers using a dimer receptor model. Pharmacological research, 139, 337–347. https://doi.org/10.1016/j.phrs.2018.11.032

34 Hussmann, G. P., & Kellar, K. J. (2012). A new radioligand binding assay to measure the concentration of drugs in rodent brain ex vivo. The Journal of pharmacology and experimental therapeutics, 343(2), 434–440. https://doi.org/10.1124/jpet.112.198069

35 Beam, A., & Motsinger-Reif, A. (2014). Beyond IC50s: Towards Robust Statistical Methods for in vitro Association Studies. Journal of pharmacogenomics & pharmacoproteomics, 5(1), 1000121. https://doi.org/10.4172/2153-0645.1000121

36 Brunner, F., & Kukovetz, W. R. (1991). Radioligand binding to muscarinic receptors of bovine aortic endothelial cells. British journal of pharmacology, 102(2), 373–380. https://doi.org/10.1111/j.1476-5381.1991.tb12181.x

37 Kalliokoski T, Kramer C, Vulpetti A, Gedeck P. Comparability of mixed IC_{50} data - a statistical analysis. PLoS One. 2013;8(4):e61007. Published 2013 Apr 16. doi:10.1371/journal.pone.0061007

38 Lazareno, S., & Birdsall, N. J. (1993). Estimation of competitive antagonist affinity from functional inhibition curves using the Gaddum, Schild and Cheng-Prusoff equations. British journal of pharmacology, 109(4), 1110–1119. https://doi.org/10.1111/j.1476-5381.1993.tb13737.x

39 Kilian, J., Ozenil, M., Millard, M., Fürtös, D., Maisetschläger, V., Holzer, W., Wadsak, W., Hacker, M., Langer, T., & Pichler, V. (2022). Design, Synthesis, and Biological Evaluation of 4,4'-Difluorobenzhydrol Carbamates as Selective M1 Antagonists. Pharmaceuticals (Basel, Switzerland), 15(2), 248. https://doi.org/10.3390/ph15020248

40 Lau, J., Rousseau, E., Kwon, D., Lin, K. S., Bénard, F., & Chen, X. (2020). Insight into the Development of PET Radiopharmaceuticals for Oncology. Cancers, 12(5), 1312. https://doi.org/10.3390/cancers12051312

41 Pajouhesh H, Lenz GR. Medicinal chemical properties of successful central nervous system drugs. NeuroRx. 2005 Oct;2(4):541-53. doi: 10.1602/neurorx.2.4.541. PMID: 16489364; PMCID: PMC1201314.

42 Ozenil M, Skos L, Roller A, Gajic N, Holzer W, Spreitzer H, Platzer-Ozenil S, Vraka C, Hacker M, Wadsak W, Pichler V. Unexpected scaffold rearrangement product of pirenzepine found in commercial samples. Sci Rep. 2021 Dec 3;11(1):23397. doi: 10.1038/s41598-021-02732-y. PMID: 34862437; PMCID: PMC8642400.

43 Kilian J, Millard M, Ozenil M, Krause D, Ghaderi K, Holzer W, Urban E, Spreitzer H, Wadsak W, Hacker M, Langer T, Pichler V. Synthesis, Biological Evaluation, and Docking Studies of Antagonistic Hydroxylated Arecaidine Esters Targeting mAChRs. Molecules. 2022 May 16;27(10):3173. doi: 10.3390/molecules27103173. PMID: 35630651; PMCID: PMC9145622.

44 Ozenil M, Aronow J, Piljak D, Vraka C, Holzer W, Spreitzer H, Wadsak W, Hacker M, Pichler V. Synthesis, Biological, and Computational Evaluation of Antagonistic, Chiral Hydrobenzoin Esters of Arecaidine Targeting mAChR M1. Pharmaceuticals (Basel). 2020 Nov 30;13(12):437. doi: 10.3390/ph13120437. PMID: 33266067; PMCID: PMC7760838.

45 Ozenil M, Pacher K, Balber T, Vraka C, Roller A, Holzer W, Spreitzer H, Mitterhauser M, Wadsak W, Hacker M, Pichler V. Enhanced arecoline derivatives as muscarinic acetylcholine receptor M1 ligands for potential application as PET radiotracers. Eur J Med Chem. 2020 Oct 15;204:112623. doi: 10.1016/j.ejmech.2020.112623. Epub 2020 Jul 19. PMID: 32717485.

46 Lipinski CA. Lead- and drug-like compounds: the rule-of-five revolution. Drug Discov Today Technol. 2004 Dec;1(4):337-41. doi: 10.1016/j.ddtec.2004.11.007. PMID: 24981612.

ABBREVIATIONS

[^{3}H] NMS - [N-methyl-^{3}H] scopolamine methyl chloride

[^{3}H] QNB - [^{3}H] quinuclidinyl benzilate

AC - adenylyl cyclase

ACh - acetylcholine

BBB - blood-brain barrier

cAMP - cyclic adenosine monophosphate

CHO - chinese hamster ovary cells

clogP - calculatedlogarithm of partition coefficient

CNS - central nervous system

CPM - counts per minute

DAG - diacylglycerol

DMSO - dimethyl sulfoxide

DPBS - dulbecco's phosphate buffered saline

EDTA - ethylendiaminetetraacetic acid

ER - endoplasmic reticulum

FBS - fetal bovine serum

FDA - food and drug administration

GDP - guanosine diphosphate

GPCRs - G protein coupled receptors

GTP - guanosine triphosphate

IC_{50} - half maximum inhibition concentration

IP_3 - inositol triphosphate

K_a - equilibrium association constant

K_D - equilibrium dissociation constant

K_i - equilibrium inhibition constant

k_{off} - dissociation constant

k_{on} - association constant

L - ligand

LAF - laminar air flow

LR - ligand-receptor complex

mAChRs - muscarinic acetylcholine receptors

nAChR - nicotinic acetylcholine receptors

PEI - poly(ethyleneimine)

PET - positron emission tomography

PIP_2 - phosphatidylinositol bisphosphate

PLC - phospholipase C

PNS - peripheral nervous systems

R - receptor

rpm - revolutions per minute

Scop. - scopolamine

TRIS - tris(hydroxymethyl)aminomethane